SPARC-LS-09/001
18 May 2009

UV PULSE SHAPER: SIMULATIONS AND EXPERIMENTAL CHARACTERIZATION

C. Vicario, D. Filippetto *(INFN/LNF)*

Abstract

To optimally drive the SPARC photoinjector a flat top laser pulse with short rise time and variable length is requested. To control these features an optical system has been designed, constructed and tested. The apparatus is a UV stretcher installed after the third harmonics generator upstream the optical transfer line to the SPARC photocathode gun. The stretcher is composed by two efficient transmission gratings. Two lenses inserted between the gratings, focus the laser at a particular plane where there is a full correlation between the transverse position and the optical wavelengths. At this plane it is possible to introduce a proper mask to perform an amplitude spectral modulation and improve the pulse rise time. The relative distance between the gratings allows also the control of the final pulse length. This feature is particular useful to produce different e-beam current and explore different working points for the SPARC photoinjector. In this note we will describe the UV stretcher and will present some experimental measurements to characterize the apparatus.

1 SPARC LASER SYSTEM

The SPARC laser system is used to produce high density electron bunch from a RF-gun photocathode. The laser system is synchronized with the accelerating field in order to extract the beam at the optimal phase. To maximize the beam brightness, the laser beam is required to have uniform transverse profile. Finally, for optimally drive a S-band RF gun, a relatively high energy (>100 μJ) UV laser pulse is needed, with a flat top temporal profile between 5 to 12 picoseconds and fast (about 1 ps) rise and fall time [1-3].
The SPARC laser system, see figure 1, is based on a Ti:Sa oscillator that generates 130 *fs* pulses with a repetition rate of 79+1/3 MHz, the 36th sub-harmonic of the photoinjector accelerating frequency at 2856 MHz [4, 5]. An acousto-optic programmable dispersive filter called "DAZZLER," [6] used to modify the spectral amplitude and phase function, is placed between the oscillator and the amplifier. The filter modulates the spectral components in order to obtain the target temporal flat top profile at the laser exit. The amplification process is carried out by one regenerative pre-amplifier pumped by 7 W frequency doubled Nd:YLF laser and a two double passes stages which are excited by the second harmonic of a Nd:YAG with an energy of 0.5 J per pulse. The system is capable to deliver pulses with energy up 50 mJ at λ=800 nm and repetition rate of 10 Hz. Usually the amplifier output energy is kept at lower value (about 20 mJ) in order to limits non linear effect in the laser pulse propagation.

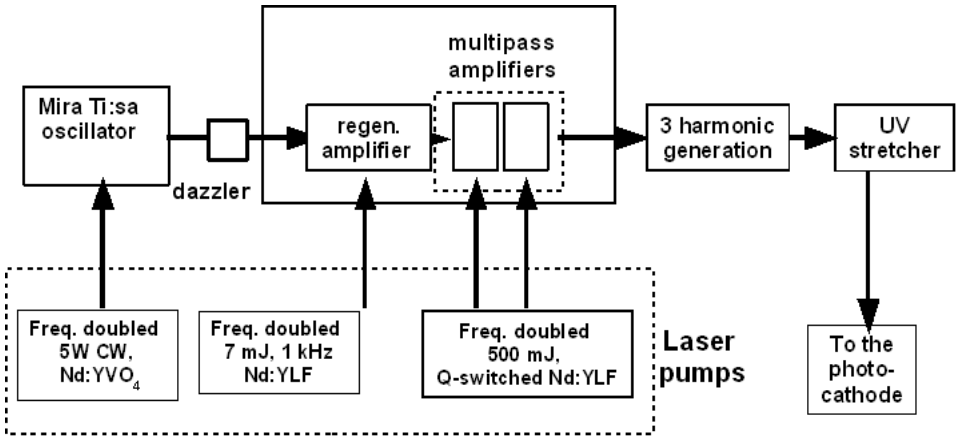

Fig 1 Laser system layout.

At the output of the amplifier the IR pulses undergo to the third harmonic generator (THG). The up-conversion is required to generate photons with energy larger than the Cu cathode work function. The third harmonic generator is composed by two type-I beta barium borate (BBO) crystals of 0.5 and 0.3 μm respectively: the first crystal generates the second harmonic signal and in the second BBO the third harmonic is achieved.
After the harmonic generation, to lengthen the pulse, an UV stretcher is installed. In this way the IR pulse length at the entrance of the THG can be constant, and consequently the laser power can be set to maximize the harmonic conversion (up to 10%). After the stretcher the central part of the laser beam is selected trough a circular aperture to obtain a top hat laser spot. Then the laser is imaged ten meters away on the photocathode by a proper optical system.

To produce the requested flat top time profile starting from the natural Gaussian laser pulses, active or passive systems, shapers, are employed. Current state of the art designs are based on various kinds of shapers in the IR, usually located before the amplifier thus suffering from deleterious non-linear effects introduced mostly in the amplification and the harmonic conversion [6, 7]. Another option that has been studied [8] is the use of a pulse stacker obtained by delayed replicas of an incoming laser pulse. While these different schemes promise to achieve relatively flat-top laser profiles, the major problem has been to satisfy at the same time also the tight photoinjector requirements such as very short rise and fall times and the pulse to pulse stability.
A simple approach to the generation of the flat top profile is based on the possibility of transferring the spectral features into the temporal profile when large chirp is applied through the UV stretcher.
A flat top spectrum in the third harmonic is generated using a proper modulation function by the DAZZLER [6]. This scheme presents significant drawbacks since the harmonic generation strongly affects the UV spectral shape. In fact, due to the finite bandwidth of the non-linear crystals, the steepness of the rise and fall time of the resulting flat-top pulses is not extremely sharp (about 3 ps). As shown in previous work [9] to produce faster rise time the spectral tails of the UV spectrum can be clipped. To apply this sharp edge modulation, an aperture can be placed in the stretcher in a plane where the laser wavelengths are spatially dispersed. The resulted spectrum and time profiles are then characterized by sharp tails.

2 UV SHAPER

The layout downstream the amplifier is sketched in the figure 2. In the Harmonic Generator (HG) the 20 mJ IR beam is converted to about 2 mJ UV pulse energy. The dichroic mirror separates the second harmonic (blue) from the IR and UV pulses, and the following UV mirror (M1) separates the IR from the UV. M3 is a periscope mirror. The UV beam changes both its height (from 17 to about 15 cm respect to the optical table plane) and its polarization (from P to S, to maximize the grating efficiency). The entrance in the stretching system is performed via the M5 mirror, allowing the input beam to make an angle of about 103 degrees respect to the output beam.
The stretching system consists of two transmissive diffraction gratings (G1 and G2) mounted anti-parallel to compensate the relative dispersion. The two lenses (L1 and L2) have a focal length of 50 cm producing a beam waist in the region between M6 and M7. In this plane (Fourier Plane) each frequency component has a waist in a slightly different horizontal position, so that the resulting beam spot has an horizontal line-like waist, with a linear correlation between space and frequency. This plane is used to perform frequency shaping.
The two UV gratings are made by *Ibsen Photonics* with 4500 grooves/mm ruled on 3 mm thick fused silica substrate. Each grating provides an efficiency of about 90% that leads, after 4 diffractions - two passes in the stretcher - to an overall stretcher efficiency of 65% (without the pulse shaping). The angle between the input and output beam is 103 degrees while the angle between perpendicular to the grating plane and the input beam ($\vartheta 1_{in}$) is 50 degrees (i.e. $\vartheta 1_{out}$ =27 degrees). The direct and reflected beams in the 4f stretcher have paths of different heights controlled by the M8 retro-reflector, that cross each other only at the Fourier plane.

The grating G2 is mounted, together with the mirrors M8, on a translation stage. By changing the grating position along the direction of the laser beam propagation, causes the temporal dispersion to be not completely compensated and the beam to increase its time duration. The laser beam FWHM duration can be changed from transform limited (<1ps) to 15 ps.
For the daily system alignment we use the 3 irises (I1, I2, I3) as reference. The horizontal alignment is also carried out by looking at the spectrometer CCD camera. The undiffracted output beam passing through G1 is focalized on the CCD, giving the spectrum image. If a beam cut at the Fourier plane is applied this will be directly visible on the spectrum and, if the back and forth beams are not horizontally superimposed on that plane, inserting a thin wire in the modulation plane leads to 2 distinct holes in the spectrum. The mirrors M8 are used to align the beams, since it only changes the back beam path.
It is worth to note that the frequency dispersion at the Fourier plane in such that 1 nm bandwidth is projected over 3.47 mm.
Moreover a deviation of the two gratings from the anti-parallel situation lead to spatial chirp and temporal distortion on the output beam. This effects have to be corrected by changing the grating angle. This is usually done focalizing a small fraction of the output beam on a CCD, and looking for some correlation between the frequency cut at the Fourier plane inside the stretcher and the transverse spot deformations.
To measure the 10Hz laser pulse time of arrival the un-diffracted beam from G2 is sent to a photodiode. From the photodiode and the successive manipulation a proper signal is extracted and mixed with the SPARC master clock. The mixing provide a direct measurement of the laser-to-RF time jitter demonstrating a phase noise within 0.5 ps rms[10].

Spectrometer

As said before after the second pass in the stretcher the un-diffracted beam is used for on-line spectrum diagnostic. These rays, in fact, propagates with an angle linearly dependent on the wavelengths. A proper focusing lens, placed at the focal distance from the grating, can be used to focus each wavelength in different positions on a CCD screen. On the sensor, the spectrum is projected along the diffraction direction and can be recorded realizing in such a way an easy-to-use spectrometer. The resolution of the spectrometer and the pixel-to-wavelength calibration can be calculated using the grating equation:

$$\beta(\lambda) = \arcsin\left(\frac{\lambda}{d} - \sin\alpha\right) \qquad (1)$$

Where β is the diffracted angle, α in the incident angle, λ and d are the wavelength and the grating's groove spacing.

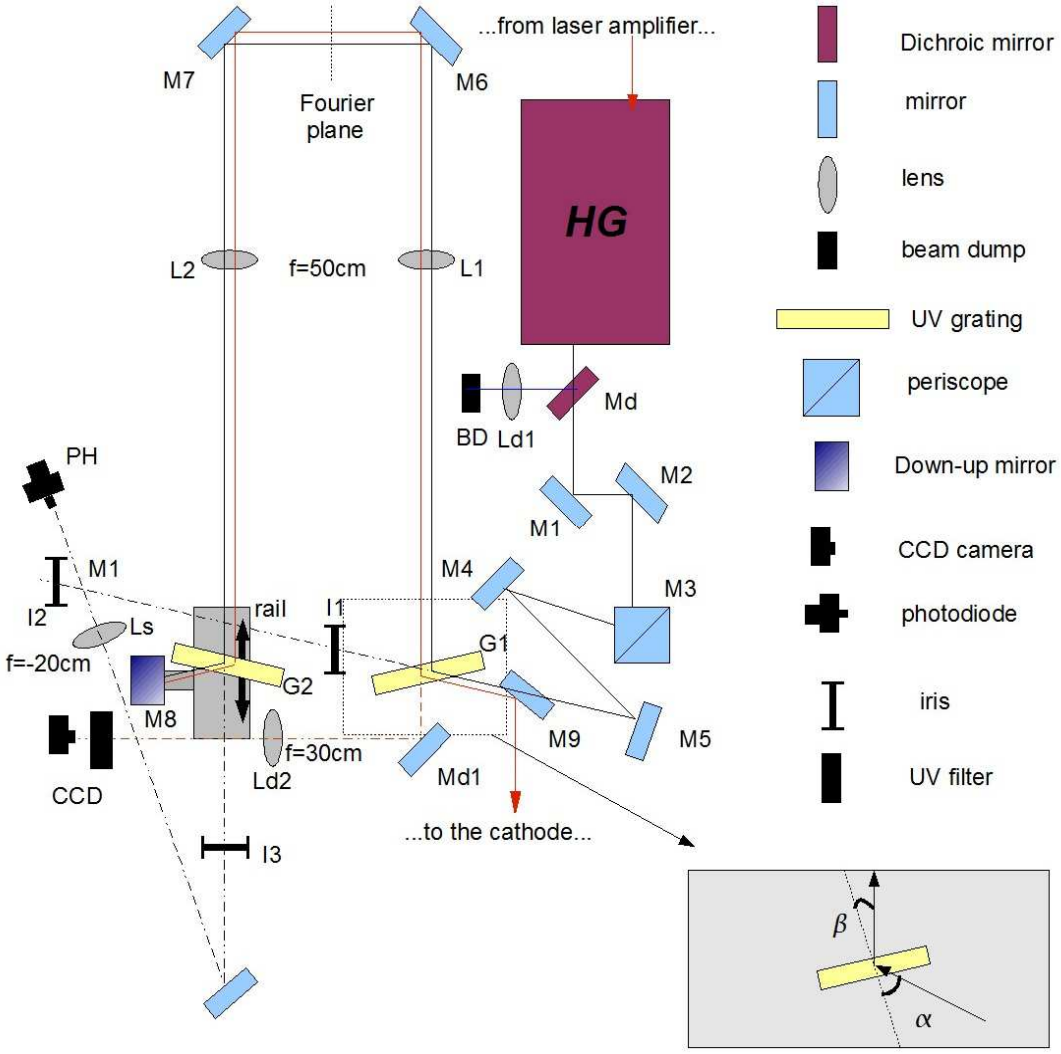

Fig 2: UV pulse shaper layout.

At the lens focal plane the laser spectrum will be dispersed by a quantity:

$$R = \left.\frac{d\beta}{d\lambda}\right|_{\lambda_0} \cdot F \cdot \Delta\lambda \qquad (2)$$

For the experimental setup, F=30 cm and α=26° we obtain R / Δλ = 2.08 mm/nm. In this condition the dimension of the CCD pixel, 9.9 μm, corresponds to a spectral width of about 0.05 A. In is important to note that this value does not set the actual spectrometer resolution since at the focus, the minimum spot size for a single wavelength can be estimated in the order of few pixel. Therefore a more realistic estimation for the spectrometer resolution is 0.2-0.3 Angstrom that is enough for the pulse shaping studies.

3 SIMULATION AND TOLERANCE STUDIES

In this paragraph the performances of the stretcher are simulated using Zemax a professional software code for optical system design [11]. The optical path for the different wavelengths is calculated in order to define the stretching factor and the final pulse length.
It is important to stress that the performances of the stretcher are strongly influenced by alignment error. In this paragraph we analyze the distortions introduced when the second grating deviate from an angle complementary to the first one.

3.1 Stretching factor

As described before the output pulse length is controlled by varying the relative position between the second grating and the second lens. In the fig 3.1 it is reported the stretching factor expressed in picosecond per nanometer of bandwidth. The red and the black points are calculated by Zemax simulation and by the analytical formula respectively. The pulse broadening is calculated with Zemax using the optical path length difference for 1 nm spectrum centered at the 266.6 nm.
Note that the same pulse length can be achieved moving the grating away or more close respect to the lenses. In this way the chirp sign is changed but the pulse length is equal. Another consideration is that the actual stretching factor depends on the sum distance of both gratings respect to the zero dispersion position. The two distances are additive for the stretching factor.

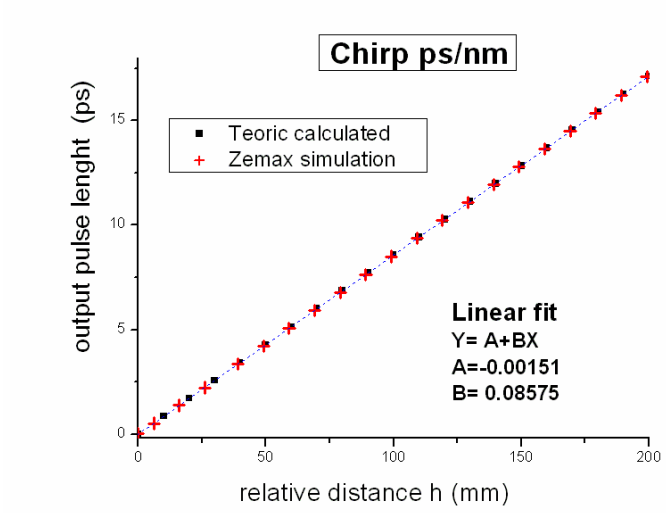

Fig 3 Output pulse duration as function of the relative distance of the grating respect to the zero dispersion position, for 1 nm laser bandwidth.

From the above calculation the pulse broadening can be estimated in the order 875 fs per cm for 1 nm bandwidth (assuming the typical laser UV bandwidth of 1.2 nm, the stretching factor is about 1 ps per cm of stretcher length). The output pulse length can be also calculated using

the following formula for the chirp introduced:

$$\Gamma = \left(\frac{\lambda^3 h}{\pi c^2 d^2} \right) \frac{1}{1 - \left(\frac{\lambda}{d} - \sin(\alpha) \right)^2} \qquad (3)$$

c is the speed of light, *d* is the grating groove spacing, α is the input angle and *h* is the relative stretcher length respect to the zero dispersion position. The output pulse length is Γ multiply by the optical frequency bandwidth Δω. In the figure 3 the black points are calculated using this formula and are in excellent agreement with the Zemax simulation.

3.2 Error on the relative angle of the gratings

The stretcher is conceived to introduce an angular dispersion and a differential optical path function on the input wavelengths. After the second pass, the angular dispersion is completely compensated. If the two gratings are at the right angle the output wavelengths overlap perfectly and the output intensity fronts results to be perpendicular to the propagating direction. Ideally the two gratings should be anti-parallel: the diffraction angle at the first grating β_1, should be equal to the input angle α_2 for the second one, consequently we can easily see that $\alpha_1 = \beta_2$. When the gratings deviate from these ideal angles the output intensity profile resulted tilted (the time of arrival is function of the transverse position). In the figure 4 we report some Zemax simulations to show the effect of misalignment of the second grating of ±2 degrees. The stretcher length is set to achieve 10 ps starting from an input spectrum of 1.2 nm.

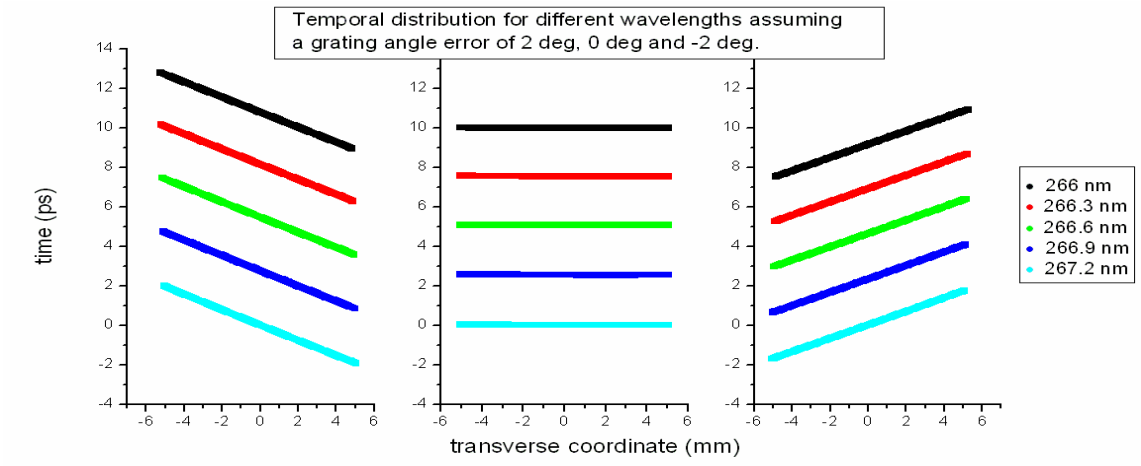

Fig 4 Effects on the output intensity front when the second grating deviate from the ideal angle.

As shown in figure 4, for 2 degree misalignment, the output time profile is significantly distorted resulting in a lack of control on sharp rise and fall time. The above pulse deformation cannot be easily revealed with standard optical diagnostic (one should for instance repeats pulse length measurement for different spot size). As secondary effect, the

angular mismatch induces also a spatial chirp on the outgoing beam; in fact along the diffraction plane the different wavelengths are shifted across the beam size with different angle. If a spatially chirped beam is focus with a converging lens, at the focal plane the spot is elliptical and the optical wavelengths are shifted in the diffraction plane. In the figure 5 it is reported the Zemax simulation for laser the wavelength distribution at the focal plane of a 100 cm lens, used in the experimental setup. The laser temporal distribution is displayed as function of transverse coordinate and for discrete wavelengths. In the simulation it has been assumed a stretcher length in order to achieve 10 ps pulse.

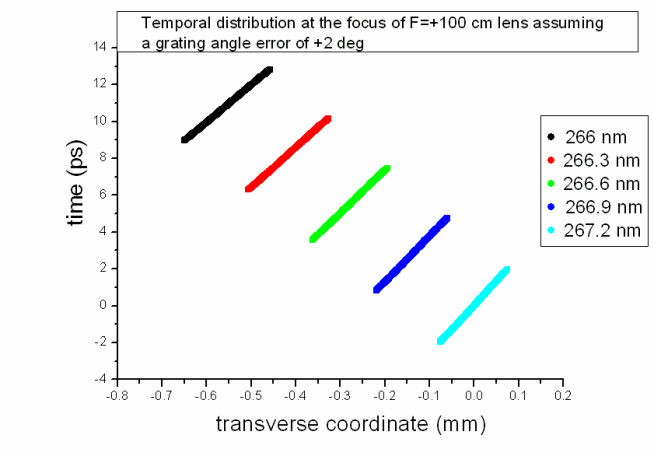

Fig 5 Effects on the output intensity front at the focus of a F=100 cm lens, when the second grating deviate of 2 degrees from the ideal angle.

As shown in the figure 5, the wavelengths are spatially separated. Using a CCD camera it is possible to measure the chirp and the misalignment of the system with great precision.

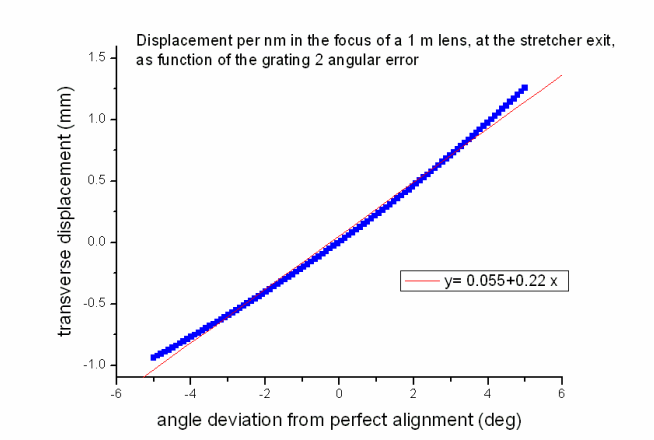

Fig 6 Distance between two wavelengths spaced by 1 nm at the focus of 1 m positive lens. The relative position is plotted as function of the grating misalignment angle.

Moreover if an obstacle is inserted in the Fourier plane, it is immediately visible on the CCD.

To quantify the resolution of the presented technique for grating alignment, it has been performed a simulation to calculate the position shift between two wavelength spaced by 1 nm, as function of the gratings relative angular error. As reported in the figure 6 the relative distance between the two wavelengths is 0.22 mm for 1 degree of error. The resolution is therefore set by the CCD pixel dimension: 9.9 μm can be estimated in the order of 0.1 degree (2 pixels). According to simulation this error introduces an acceptable pulse distortion on the rise time of about 100 fs.

4 EXPERIMENTAL MEASUREMENTS

4.1 Stretcher wavelength-to-time calibration

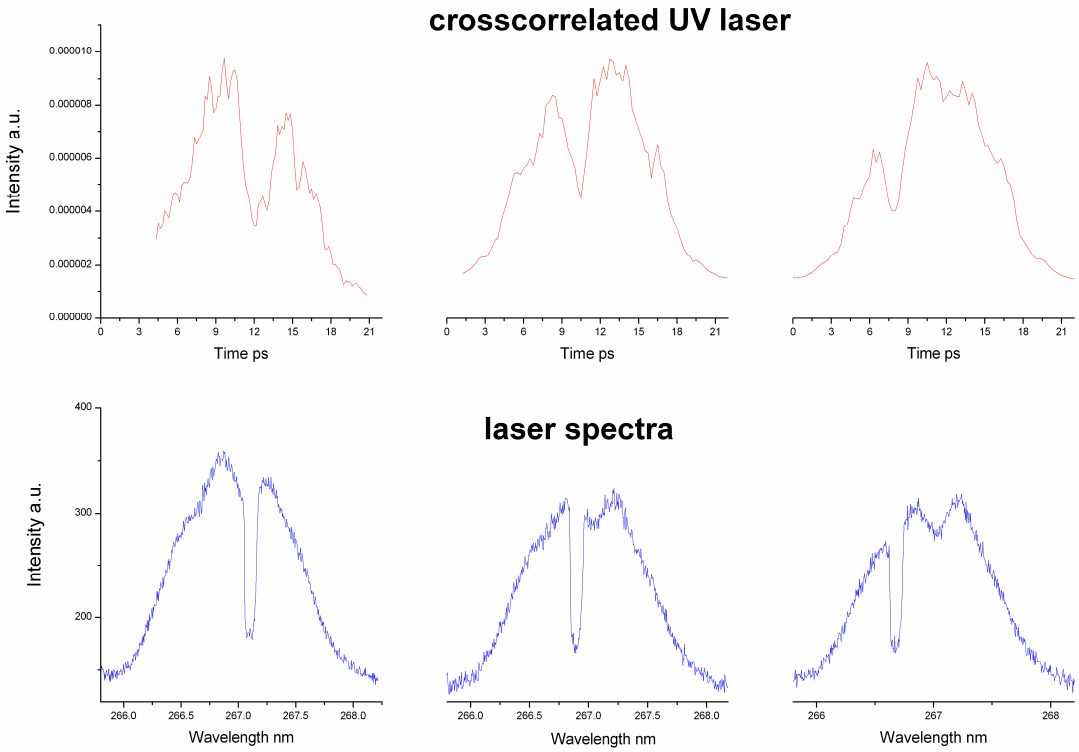

Fig 7 cross-correlated intensity (red curve) and the corresponding spectra (blue) when a thin wire is moved across the Fourier plane

The behavior of the UV stretcher as shown before can be calculated and simulated. This allows to predict the characteristic of the output pulse length: for instance it is possible on shot-to-shot base to retrieve the temporal profile using the spectrometer. Anyway a direct

measurement between the temporal and the spectral intensity for a given stretcher length is useful to qualify the apparatus.
The calibration procedure we adopted consists of inserting a thin wire at the Fourier plane and move it across the beam. For different positions of the wire we recorded the spectrum and the cross-correlation, figure 7. Extracting the position of the hole in the spectrum and in the temporal profile it is possible to determine the wavelength to time conversion. For the measurement the relative stretcher length *h* for a grating position of 12.5 cm

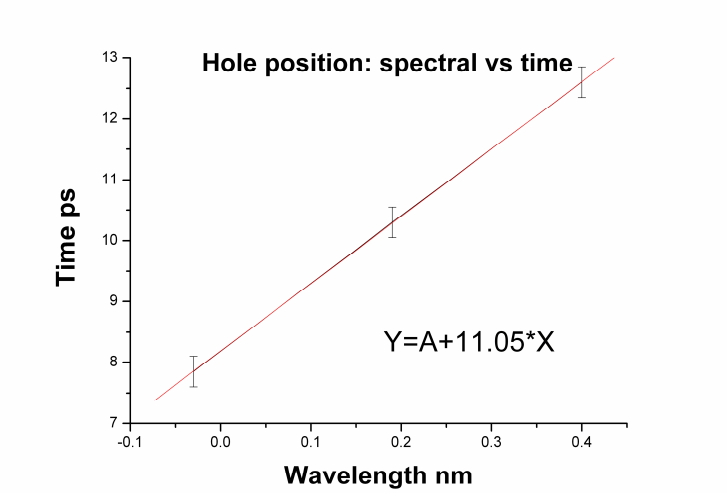

Fig 8 Wavelength-to-temporal calibration: experimental points and linear fit using the data

In the figure 8, the position of the hole in time and in the wavelength domain are reported. It is evident there is a good linear fit, the error bars correnspond to the time step of the cross-correlator. The conversion factor is 11 ps per nm, this number is in agreement with the one that can be calculated with the fit in the figure 3, that corresponds to 10.7 ps /nm.

2.1 From Gaussian to flat top

As reported before, the generation of the flat top pulse can be achieved by cutting the tails of the spectral intensity. In fact, at the stretcher exit the time shape is very similar to the spectral one. Therefore the rise time can be improved by sharp cut of the edge of the spectrum generated with the DAZZLER only shaper. It is important to stress that a strong filtering reduces the spectral components and increase the energy losses. In this condition, due to smaller bandwidth, the resulted rise time is worsen. As a rule of thumb the rise time for a fixed pulse length is proportional to the square root of the spectral width [9]. There is a best condition that can be sought for the shortest rise time. In the figure 9, the spectral and the cross-correlated profiles recorded for different spectral cuts are reported. It is visible the strong similarity the spectral and the temporal shape.

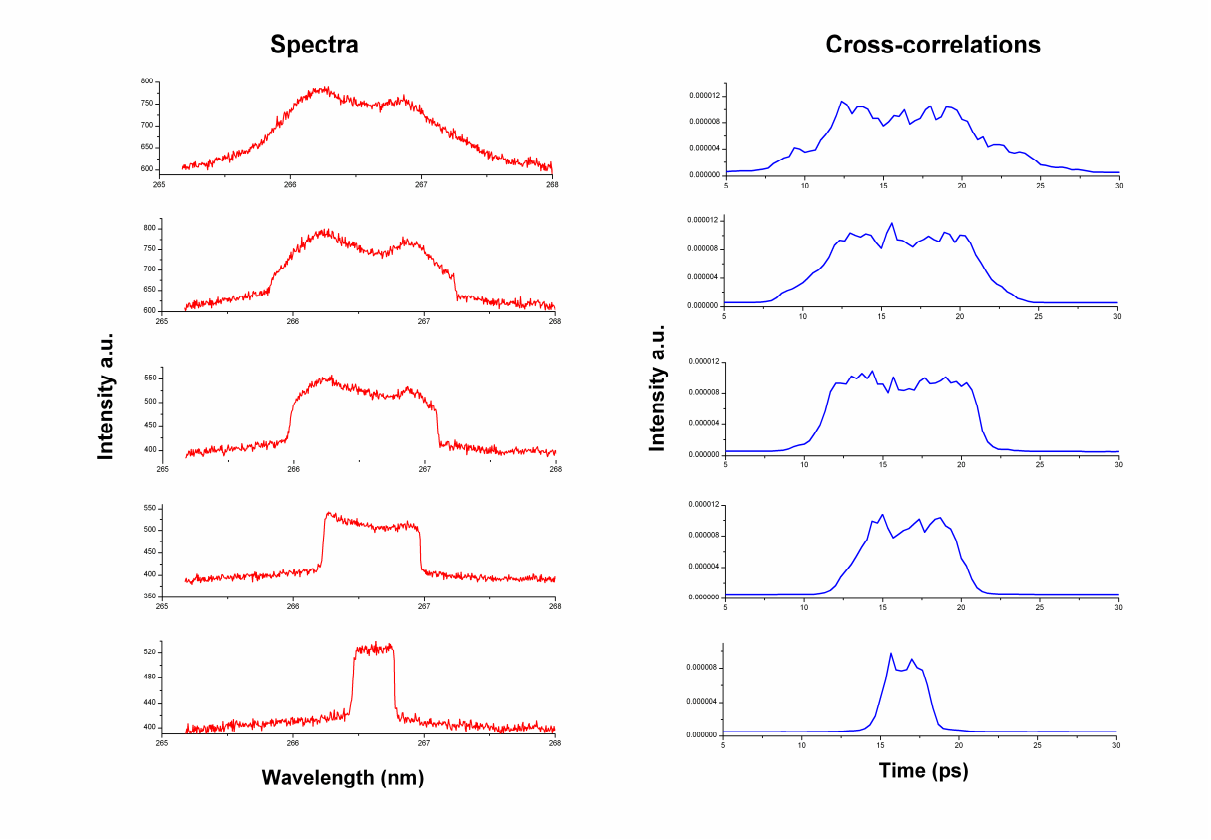

Fig 9 Pulse shapes obtained for different spectral cut in the stretcher. On the left are reported the spectra and on the right the corresponding cross-correlated profile.

In the first row it is reported the shape obtainable without spectral modulation in the stretcher. The DAZZLER is used to generate a super-Gaussian profile in the spectrum and therefore in time. The rise time is more than 3 ps. A gentle spectral cut (second row) induces a slightly improvement in the rise time. But when further spectral cut is applied the pulse's steepness significantly improves: the best square profile is shown in the central row. The resulted rise time is less than 1.4 ps and the ripple on the plateau is within 10 % rms. The energy losses due to the spectral filtering can be estimated by integration of the spectra and results to be about 20%.
In the last two rows it is shown that when the spectral width is strongly reduced the time profile became less squared (the ratio between rise time and pulse length increases).

2.2 **Multipeaks pulse shape**

The generation of multipeaks laser pulse is of great interest for a wide variety of coherent radiation source. In electron photoinjectors, fluctuations in the charge density resulting from the drive laser can be amplified and converted to energy spread as the beam is accelerated. During subsequent beam manipulation stages, such as injection bends or compression, these perturbations may result in current modulation and in the production of coherent radiation.

The multipeaks shape can be obtained applying a periodic filter at the Fourier plane in the UV stretcher. In the figure 10 it is reported the UV laser pulse measured at the stretcher exit with a sub-ps resolution streak camera (red curve). This pulse has been produced by introducing at the Fourier plane a mask composed by three wires, 200 microns thick. The recorded shape is compared with the calculate inverse Fourier transform of the measured spectrum considering also the chirp introduced on the laser pulse. The simulated and measured curve perfectly overlap.

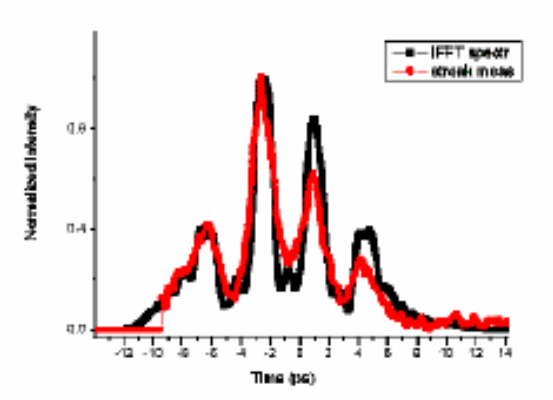

Fig. 10 Multipeaks pulse obtained by inserting hre thin wires in the stretcher Fourir plane

The generation of few peaks laser shape can be easily accomplished using the present scheme. As more micro-pulses are required the present technique becomes ineffective. In fact, the spectral width of single micro-pulse would be too narrow and the corresponding time profile would enlarge and overlap with the neighbor micro-pulses. Many micro-pulses shape should be synthesized adopting different schemes.

3 CONCLUSIONS

In this report we described the UV stretcher optical system. This device was conceived to produce high energy pulse with pulse length variable over several picosecond. Applying a proper amplitude modulation in the plane were the frequency are dispersed it is possible to generate flat top or multipeaks UV pulses. In this report we simulated the performances of the stretcher and the effect of not perfect alignment. Finally some example of experimental pulse shapes are reported.

4 REFERENCES

[1] J. Yang, F. Sakai, T. Yanagida, M. Yorozu, Y. Okada, K. Takasago, A. Endo, A. Yada, M. Washio, J. Appl. Phys. **92**, 1608 (2002).

[2] L. Palumbo and J. Rosenzweig, eds., *Technical Design Report for the SPARC Advanced Photo-Injector* (Laboratori Nazionali Frascati, Istituto Nazionale di Fisica Nucleare, 2004).

[3] P. R. Bolton and J. E. Clendenin, Nucl. Instrum. Methods Phys. Res. A **483**, 296 (2002).

[4] S. Cialdi, M. Petrarca and C. Vicario, Opt. Lett. Vol 31, (2006), 2885, and Virtual Journal of Ultrafast Science Oct. 2006.

[5] M. Bellaveglia, C. Vicario, A. Drago, A. Gallo, A. Ghigo, L. Cacciotti, G. Gatti, P. Musumeci, M. Petrarca: "Laser Timing and Synchronization Measurements", LS-06/001, 01/02/2006

[6] F. Verluise, V. Laude, J.P. Huignard, P. Tournois, A. Migus, J. Opt. Soc. Am. B, 17, 138 (2000).

[7] A. M. Wiener, Rev. Sci. Instr., **71**, (2000), 1929.

[8] H. Dewa et al., Proceeding FEL Conference 2006, THPPH034, http://www.jacow.org.

[9] C. Vicario, M. Petrarca, S. Cialdi, P. Musumeci: "High-power Third-harmonic Flat Laser Pulse Generation", LS-07/001, 23/05/2007

[10] A. Gallo, D. Alesini, M. Bellaveglia, G. Gatti and C. Vicario et al., Performances of the SPARC Laser and RF Synchronization Proceedings of EPAC THPC156, Genoa, Italy 2008.

[11] http://www.zemax.com/